

Performance Analysis of IEEE 802.11 Distributed Coordination Function in Presence of Hidden Stations under Non-saturated Conditions with Infinite Buffer in Radio-over-Fiber Wireless LANs

Amitangshu Pal and Asis Nasipuri

Electrical & Computer Engineering, The University of North Carolina at Charlotte, Charlotte, NC 28223-0001

E-mail:{apal, anasipur}@uncc.edu

Abstract- We present an analytical model to evaluate the performance of the IEEE 802.11 Distributed Coordination Function (DCF) with and without the RTS/CTS handshake in radio-over-fiber (RoF) wireless LANs. The model captures the effects of contending nodes as well as hidden terminals under non-saturated traffic conditions assuming large buffer sizes. The effect of fiber propagation delay is considered. The proposed models are validated using computer simulations. Comprehensive performance evaluations of RoF networks obtained from the proposed model as well as simulations are presented.

Keywords: Radio-over-fiber, IEEE 802.11, hidden stations, non-saturated traffic.

I. INTRODUCTION

Radio over fiber technology has attracted significant attention in recent times as a promising approach for providing improved wireless coverage at a low cost in broadband access networks. RoF utilizes high bandwidth optical links to distribute radio frequency (RF) signals from a central unit to remote antenna units (RAU) that may be distributed over a wide region. Fig. 1 illustrates the basic architecture of a typical RoF network. For the downlink, the electrical signal generated by an *access point* (AP) is converted to optical (E/O conversion) and sent through the optical link to the corresponding RAU. At the antenna, this is converted into a radio signal and transmitted to the wireless nodes. The reverse happens for the uplink where the RF signals from wireless nodes are converted into optical (E/O conversion) at the antenna and sent over the optical link to the central unit, where it is converted back to electrical signal.

Using RoF for wireless coverage has numerous advantages. In RoF networks, all complex and expensive equipment, such as those required for modulation and switching, are located at the central unit. The only functions carried out at the RAUs are the RF amplifications and optical to electrical conversion and vice versa. This enables the RAUs to be simpler and less expensive, which reduces the overall installation and maintenance costs. The large bandwidth and low attenuation of optical fiber offers high capacity for transmitting radio signals. Also, including optical fibers reduce problems related to interference, as optical fiber cables are insensitive to electromagnetic radiations. In addition, this simpler RAU with low-complexity equipment results in reduced power consumption.

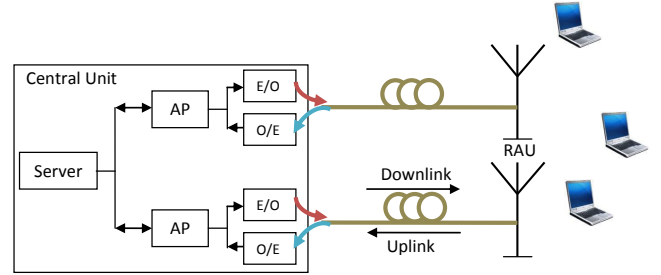


Fig. 1. Block diagram of a radio-over-fiber network

Although each AP in an RoF network can use the same channel access protocol as in other wireless LANs, the addition of the fiber link between the AP and the RAU introduces additional factors that affect the performance of the medium access control (MAC) protocol. In this paper, we analyze the performance of the IEEE 802.11 DCF in RoF networks under non-saturated traffic conditions for both the basic and the optional RTS/CTS access mechanisms. Our analysis takes into account the effects of transmissions from contending nodes, i.e. nodes contending to gain access to the channel at the same time as the source node, as well as that of hidden terminals, which might disrupt the reception of a packet if they commence transmission at any time during the receiver's vulnerable period. In addition, as opposed to other existing literature on the analysis of DCF performance, we assume large buffer sizes, which is a more realistic assumption for accurate computation of the total delay (MAC plus queuing delay). Moreover, we consider the effect of the fiber length, which adds an extra propagation delay and poses a challenge to the system design of IEEE 802.11.

II. RELATED WORK

A significant amount of work has been reported on the performance analysis of 802.11 systems. The pioneering work by Bianchi in [1] presents a two-dimensional Markov chain model that effectively captures the performance of IEEE 802.11 DCF under saturated traffic conditions. However, it does not consider the effect of hidden stations. The authors of [2] extend Bianchi's model to obtain the performance under non-saturated traffic conditions, without capturing the effects of hidden nodes. The throughput performance with hidden nodes

under saturated traffic condition with RTS/CTS is presented in [3], whereas in [4] the authors discussed the effects of hidden terminals in non-saturated traffic conditions to measure the throughput performance. The delay performance in 802.11 DCF is also well researched. In [5] [6] the delay performance in the presence of only contending stations and saturated traffic conditions are presented. In [7], the authors propose a model based on Bianchi's model to calculate delay in presence of hidden stations and in non-saturated traffic condition. All of the above literature consider short buffer sizes, which does not capture the effect of queuing delay properly. The impact of large buffer is considered in [8] where the authors model the throughput and total delay in absence of hidden stations. The saturated throughput performance of DCF in RoF is addressed in [9] in the absence of hidden nodes, where the effect of buffering is ignored as well.

In this paper, our main contributions are as follows. First, we extend the model in [2], [4], [8] to include the effect of hidden stations with infinite buffer in the basic IEEE 802.11 DCF and that using RTS/CTS for radio-over-fiber wireless networks. We also evaluate the total delay, which includes the queuing delay. We validate our analytical model by using simulations in ns-2. Finally, we address the effect of fiber propagation delay on network throughput and probability of collision. To the best of our knowledge, this is the first paper that addresses the performance evaluation of IEEE 802.11 MAC in presence of hidden stations with large buffer and nonsaturated condition in RoF networks.

III. MODELING OF IEEE 802.11 DCF IN RoF WIRELESS LANs

In this section we present the analytical model of the IEEE 802.11 DCF in RoF wireless LANs, taking into account non-saturated traffic conditions, the effects of contending and hidden stations, infinite buffers and fiber propagation delay.

A. Modeling of Nonsaturated Stations

According to the IEEE 802.11 standard, the contention window, also called the backoff window, increases exponentially from a minimum size W_0 to the maximum size W_{max} as follows:

$$\begin{aligned} W_i &= 2^i W_0 \quad 0 \leq i \leq m \\ &= 2^m W_0 = W_{max} \quad i > m \end{aligned} \quad (1)$$

Here m is the backoff stage at which the contention window reaches the maximum value W_{max} , where it remains in successive stages as well. In [1], Bianchi presents a Markov model to describe this backoff window size where each station is modeled by a pair of integers (i, k) . The back-off stage i starts at 0 at the first attempt to transmit a packet and is increased by 1 every time a transmission attempt results in a collision, up to a maximum value of m . It is reset after a successful transmission. The counter k is initially chosen uniformly between $[0, W_i - 1]$, where $W_i = 2^i W_0$ is the range of the counter. The counter is decremented when the medium is idle. The station transmits when $k = 0$.

The above model was extended to address nonsaturated traffic conditions in [2] and [8]. The authors assume a constant probability q of at least one packet arriving during the average slot time on the medium. They also assume the following terms: the probability that a packet is available to the MAC immediately after a successful transmission, denoted by r ; the probability of collision, denoted by p ; and the probability of transmission in a randomly chosen slot, denoted by τ . Our analysis is based on a similar approach; however, we also consider the effect of large buffer and fiber propagation delay. In this subsection, we first analyze the effect n contending stations (i.e. no hidden station).

Following the derivations presented in [2] and [8], the packet transmission probability τ in a generic slot time can be written as:

$$\tau = \frac{1}{\eta(1-r)} \left(\frac{q^2 W_0}{(1-p)(1-(1-q)^{W_0})} - rq(1-p) \right) \quad (2)$$

where η can be found by:

$$\begin{aligned} \eta &= (1-q) + \frac{q^2 W_0 (W_0 + 1)}{2(1-(1-q)^{W_0})} + \\ &\frac{q(W_0 + 1)}{2(1-r)} \left(\frac{q^2 r W_0}{1-(1-q)^{W_0}} + qp(1-r) - qr(1-p)^2 \right) \\ &+ \frac{p}{2(1-r)(1-p)} \left(\frac{q^2 W_0}{1-(1-q)^{W_0}} - rq(1-p)^2 \right) \times \\ &\left(2W_0 \frac{1-p-p(2p)^{m-1}}{1-2p} + 1 \right) \end{aligned} \quad (3)$$

Note that τ depends on the values of p , q , and r . The probability of collisions p is equal to the probability that at least one of the $n-1$ remaining stations transmit in that slot. Thus

$$p = 1 - (1-\tau)^{n-1} \quad (4)$$

We assume that packets are generated in each node according to a Poisson arrival process with exponentially distributed inter-packet arrival times with rate λ_g . When an infinite buffer size is considered, the collided packets will be retransmitted. Consequently, the rate at which packets arrive in the queue is given by

$$\lambda = \lambda_g + \lambda_g p + \lambda_g p^2 + \dots = \frac{\lambda_g}{1-p} \quad (5)$$

With these, the probability of a packet arrival in a slot can be expressed as

$$q = 1 - e^{-\lambda T} \quad (6)$$

Here, T is the average slot time, which can either be empty, include a successful transmission, or have a collision. These can occur with probabilities $1 - P_{tr}$, $P_{tr}P_s$ and $P_{tr}(1 - P_s)$ respectively, where P_{tr} represents the probability that there is at least one transmission in a time slot and P_s denotes the probability of success. Hence,

$$T = (1 - P_{tr})\sigma + P_{tr}P_s T_s + P_{tr}(1 - P_s)T_c \quad (7)$$

where σ is the duration of an empty time slot, T_s is the average time the channel is sensed busy because of a successful

transmission, T_c is the average time the channel is sensed busy by each station during a collision. The expressions of T_s and T_c are presented in the next subsection.

Also, P_{tr} can be written as:

$$P_{tr} = 1 - (1 - \tau)^n \quad (8)$$

The probability of success P_s is given by the probability that exactly one station transmits, conditioned on the fact that there is at least one transmission in the channel, i.e.,

$$P_s = \frac{\binom{n}{1} \tau (1 - \tau)^{n-1}}{P_{tr}} = \frac{n \tau (1 - \tau)^{n-1}}{1 - (1 - \tau)^n} \quad (9)$$

As mentioned earlier, r is the steady state probability that a M/G/1 queue has a packet awaiting in it's buffer after a service time, thus r can be written as

$$r = \min(1, \lambda_g E[d]) \quad (10)$$

where $E[d]$ is the *access delay*, which is defined as the time interval between the instant when the packet reaches the head of the transmission queue and begins contending for the channel, and the time when the packet is successfully received at the destination station. Thus $E[d]$ consists of backoff time to get access to the channel and time for successful transmission of that packet, i.e.

$$\begin{aligned} E[d] &= \bar{T}_B + T_s \\ &= \frac{T \left(W_0 \frac{1-p-2^m p^{m+1}}{1-2p} - 1 \right)}{2(1-p)} + \frac{p}{1-p} T_c + T_s \end{aligned} \quad (11)$$

where \bar{T}_B is the average backoff time (calculation is shown in Appendix A).

The nonlinear equations (2)-(11) must be solved together. To calculate the throughput, we observe that during an average slot period T , a station transmits a successful packet with a probability of $P_s P_{tr}$. Hence, for a packet payload of $E[P]$, the throughput (number of bits in unit time) is represented as

$$S = \frac{P_s P_{tr} E[P]}{T} \quad (12)$$

To calculate the total delay (including the queuing delay) of a packet, we assume an M/G/1 queue model with arrival rate of λ and service time $E[d]$. Thus the total delay of a packet is given by

$$T_d = E[d] + \frac{\lambda E[d]^2}{(1 - \rho)} \quad (13)$$

where ρ is given by $\rho = \lambda E[d]$. From [5], we can get $E[d^2]$ as

$$\begin{aligned} E[d^2] &= \text{Var}\{\bar{T}_B + T_s\} = \text{Var}\{\bar{T}_B\} \\ &= \left[\frac{T(W_0 \gamma - 1)}{2} + T_c \right]^2 \frac{p}{(1-p)^2} \end{aligned} \quad (14)$$

where

$$\gamma = \frac{[2p'^2 - 4p' + 1 - m(-1 + 2p')p'] [2p]^m + 2p'^2}{(-1 + 2p'^2)} \quad (15)$$

and $p' = 1 - p$. The delay can be calculated using equation (13) as long as $\rho \leq 1$, while $\rho > 1$ the queue becomes unstable, equation (13) does not capture this effect.

B. Modeling Hidden Stations in the 802.11 Basic Access Scheme

In the basic access scheme, T_s and T_c can be expressed as

$$\begin{aligned} T_s &= DIFS + H + E[P] + F + SIFS + T_{ACK} + F \\ T_c &= DIFS + H + E[P] + F \end{aligned} \quad (16)$$

where DIFS, SIFS are the interframe spacing length, H and T_{ACK} are the length of the header and the acknowledgement packet and F is the fiber propagation delay (discussed in section III.D). Now let us assume that there are c contending stations and h hidden stations. Hence, here the total number of stations is $n = c + h$. In this situation a packet from a contending station is successful if

- None of the remaining contending stations transmit in the same slot. This happens with a probability of $(1 - \tau)^{c-1}$.
- No hidden stations transmit during the vulnerable period of the whole DATA transmission. The vulnerable period of the whole transmission is given by $V = 2T_s$, thus the probability that h hidden stations do not transmit in the vulnerable period of the DATA transmission is given by $e^{-h\lambda_g V} = (1 - q)^{hk(1-p)}$, where k is the approximate number of slot durations in $2T_s$, i.e. $k = \frac{V}{T} = \frac{2T_s}{T}$.

Hence, here p , P_{tr} and P_s can be written as:

$$p = 1 - (1 - \tau)^{c-1} (1 - q)^{hk(1-p)} \quad (17)$$

$$P_{tr} = 1 - (1 - \tau)^c \quad (18)$$

$$P_s = \frac{c\tau(1 - \tau)^{c-1} (1 - q)^{hk(1-p)}}{1 - (1 - \tau)^c} \quad (19)$$

Similar to [4], assuming $T_s = \alpha\sigma$, $T_c = \beta\sigma$ and $V = \gamma\sigma$, and using the values of T_s and T_c from equation (16) in (7), and $T = \frac{V}{k}$, we get

$$P_{tr}[1 - \beta + (\beta - \alpha)P_s] = 1 - \frac{\gamma}{k} \quad (20)$$

Since $P_s P_{tr} = c\tau(1 - p)$ in (20), we get

$$\frac{\gamma}{k} = 1 + P_{tr}(\beta - 1) + c\tau(1 - p)(\alpha - \beta) \quad (21)$$

Finally, after rearranging (21), we get

$$k = \frac{\gamma}{1 + (1 - (1 - \tau)^c)(\beta - 1) + c\tau(1 - p)(\alpha - \beta)} \quad (22)$$

The values of p , P_{tr} and P_s obtained from the above value of k can be used to determine the network parameters as done before.

C. Modeling Hidden Stations in 802.11 with RTS/CTS

In the presence of RTS/CTS, T_s can be written as

$$\begin{aligned} T_s &= DIFS + T_{RTS} + F + SIFS + T_{CTS} + F + SIFS \\ &\quad + H + E[P] + F + SIFS + T_{ACK} + F \end{aligned} \quad (23)$$

where T_{RTS} and T_{CTS} are the length of the RTS and CTS packet respectively. The expression of T_c is more complicated.

Among the contending stations, some stations that are in the transmission range of the intended transmitter (say A) can receive the RTS/CTS, while others cannot. Let us assume that L_1 is the area that covers station A 's transmission range and L_2 is the area that covers the carrier sensing range of A , excluding L_1 . If a station X is placed in L_1 , then after receiving the RTS from X , A stays silent for a duration $T_{c1} = T_s$ even if transmission from X results in a collision. On the other hand, if X is placed in L_2 , station A waits for a shorter amount of time $T_{c2} = DIFS + T_{RTS}$ in case of a failed RTS transmission. Thus the collision duration T_c can be written as $T_c = P_{L1}T_{c1} + P_{L2}T_{c2}$, where P_{L1} and P_{L2} are the probabilities that X is placed in L_1 and L_2 .

Among the hidden stations, some stations that are within the transmission range of the intended receiver (D) receive the CTS whereas stations that are outside the transmission range of D cannot. Stations that are in the transmission range of D only collide with the RTS from A (assuming CTS transmissions to these hidden stations are successful). Thus for these stations, the vulnerable period is $V_1 = T_s + T_{RTS} + SIFS$, whereas for others (that are outside the transmission range of D) the vulnerable period is $V_2 = 2T_s$. Thus the average vulnerable period is $V = P_1V_1 + P_2V_2$, where P_1 and P_2 are the probability that a hidden station is in the transmission range of D or not. Thus, using the expressions of new T_s , T_c and V , we can calculate other parameters as done in previous subsections.

D. Effect of Fiber Propagation Delay

In RoF networks there is a fiber propagation delay between the central unit and the remote antenna, given by $F = \frac{L \text{ meter}}{2 \times 10^8 \text{ meter/secs}}$, where L is the fiber length. For pure wireless networks, $F = 0$. The ACK and CTS timeouts put a constraint on the maximum fiber length L . The transmitter should receive an ACK from the receiver within the ACK timeout ($SIFS + T_{ACK} + \text{maximum propagation delay } M$). Thus the following condition should be satisfied

$$\begin{aligned} SIFS + T_{ACK} + 2F &\leq ACK_{TO} \\ \Rightarrow F &< \frac{ACK_{TO} - SIFS - T_{ACK}}{2} = \frac{M}{2} \\ \Rightarrow L &< \frac{2 \times 10^8 (ACK_{TO} - SIFS - T_{ACK})}{2} = M \times 10^8 \quad (24) \end{aligned}$$

Similarly, if RTS/CTS is used, in order for the transmitter to receive the CTS before the CTS timeout ($SIFS + T_{CTS} + M$)

$$\begin{aligned} F &< \frac{CTS_{TO} - SIFS - T_{CTS}}{2} = \frac{M}{2} \\ \Rightarrow L &< \frac{2 \times 10^8 (CTS_{TO} - SIFS - T_{CTS})}{2} = M \times 10^8 \quad (25) \end{aligned}$$

In equations (24) and (25), ACK_{TO} and CTS_{TO} denote ACK timeout and CTS timeouts, respectively. Note that there will be no packet transmissions if equations (24) and (25) are not satisfied, and consequently, the throughput will be zero under those conditions.

IV. RESULTS AND ANALYSIS

The accuracy of the model presented above is verified by simulations using the *network simulator-2 (ns2)*. For the ease

of implementation, we assume the *transmission range* to be the same as the *carrier sensing range*. Thus $P_{L1} = P_2 = 1$ and $P_{L2} = P_1 = 0$. All stations generate packets using Poisson process and the interface queues at each nodes can store a maximum size of 2000 packets (unless otherwise mentioned). The parameters used in the simulations are listed in Table I. For all the figures in this section, the solid lines represent values obtained from analytical model and discrete points represent values from simulations. In all the figures we keep the number of colliding stations as 4 and vary the number of hidden stations denoted as h . Unless specifically mentioned, the fiber length is kept to 500 meters for the simulations.

TABLE I
SIMULATION ENVIRONMENT

Parameter	Values used	Parameter	Values used	Parameter	Values used
W_{min}	15	CTS	112 bits	RTS	160 bits
W_{max}	1023	Slot Time	9 μs	Payload Length	1000 Bytes
SIFS	16 μs	ACK	112 bits	Channel bit rate	6 Mbps
Header Duration	20 μs	DIFS	34 μs	Max propagation delay	10 μs

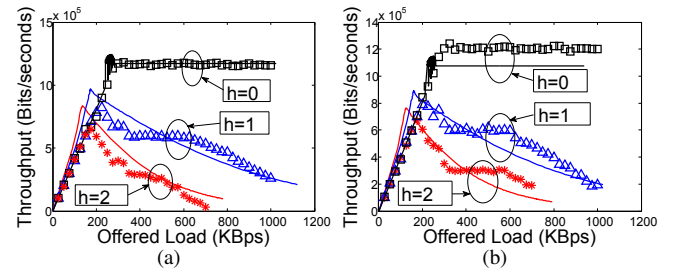


Fig. 2. Individual throughput of contending stations with different offered load (a) Basic access mechanism, (b) RTS/CTS access mechanism.

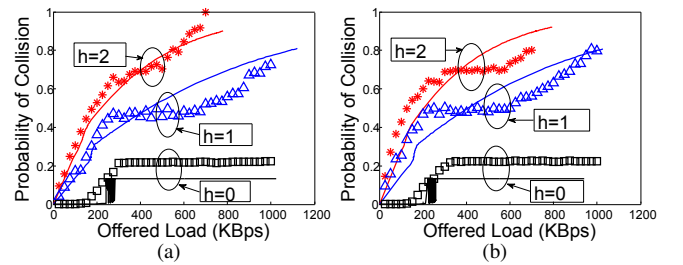


Fig. 3. Probability of Collision of contending stations with different offered load (a) Basic access mechanism, (b) RTS/CTS access mechanism.

A. Effect of Hidden Stations

Fig. 2 shows the variations of the throughputs with offered load for both the basic and RTS/CTS access mechanisms. From this figure we can observe that our analytical results match the simulation results closely. Also we can observe that at first the throughput starts increasing till it reaches a *saturation point*. After this point, in absence of hidden stations, throughput does not change with further increase in

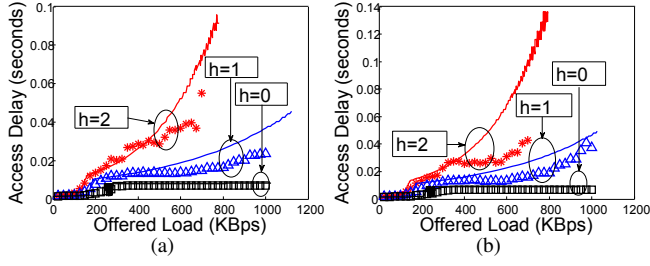


Fig. 4. Access Delay of contending stations with different offered load (a) Basic access mechanism, (b) RTS/CTS access mechanism.

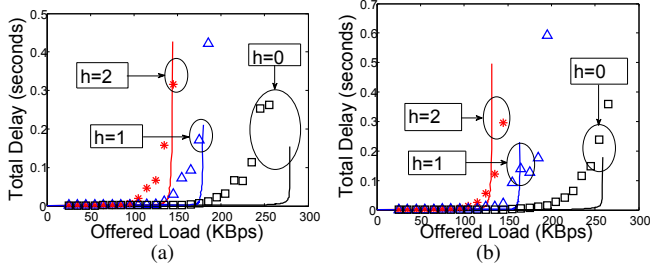


Fig. 5. Total delay of contending stations with different offered load (a) Basic access mechanism, (b) RTS/CTS access mechanism.

offered load. However in the presence of hidden stations, the throughput starts decreasing after the saturation point. This decrease in throughput is mainly because of the interference from the hidden stations at high load and due to multiple retransmissions.

Fig. 3 and 4 show the variation of the probability of collision and access delay respectively, with increasing load and different number of hidden stations. It is observed that with no hidden stations, the probability of collision and access delay get saturated after a certain offered load, while in the presence of hidden stations these parameters increase with offered load due to multiple collisions and retransmissions due to the hidden stations.

In Fig. 5, we vary the offered load and compare the total delay (queuing plus access delay) of both basic and RTS/CTS access methods and compare with those obtained using our analytical model. As mentioned in section III.A, our model is valid until $\rho \geq 1$, beyond which the queue is unstable and thus our model cannot capture that effect.

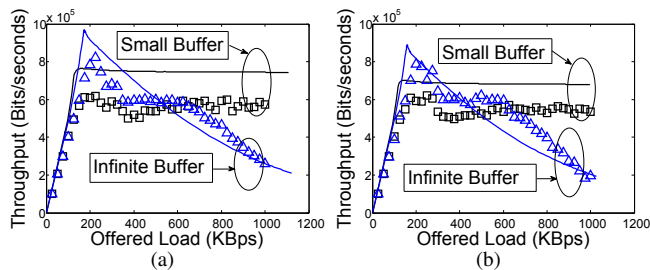


Fig. 6. Individual throughput of contending stations with different offered load (a) Basic access mechanism, (b) RTS/CTS access mechanism.

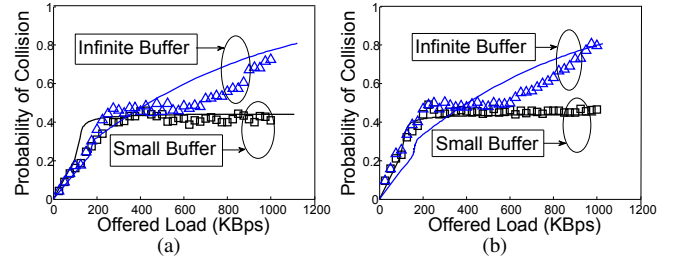


Fig. 7. Probability of Collision of contending stations with different offered load (a) Basic access mechanism, (b) RTS/CTS access mechanism.

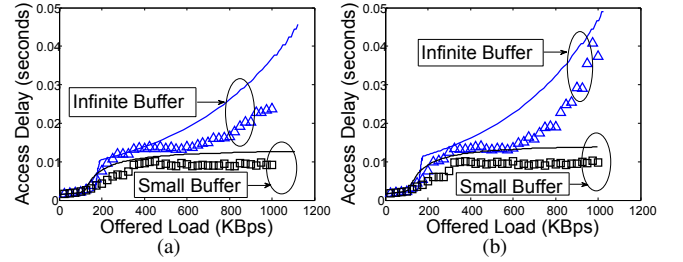


Fig. 8. Access Delay of contending stations with different offered load (a) Basic access mechanism, (b) RTS/CTS access mechanism.

B. Effect of Small and Large Buffers

Fig. 6, 7 and 8 show the variations of throughput, probability of collision and access delay with different offered load for small buffer (maximum queue length of 2 for simulation) and infinite buffer (maximum queue length of 2000 for simulation), with the number of contending and hidden stations being 4 and 1 respectively. The results for the small buffer model is based on the model presented in [4]. We observe that after certain offered load, the throughput, probability of collisions, and access delay get saturated for small buffer. This is because after a certain offered load, for small buffer, the interface queue always has a packet to transmit, causing the network parameters to be unaffected by increasing load. But for infinite buffer size, collisions, contention and retransmissions continue to increase even after the saturation point, causing the throughput to decrease, while increasing the probability of collision and access delay.

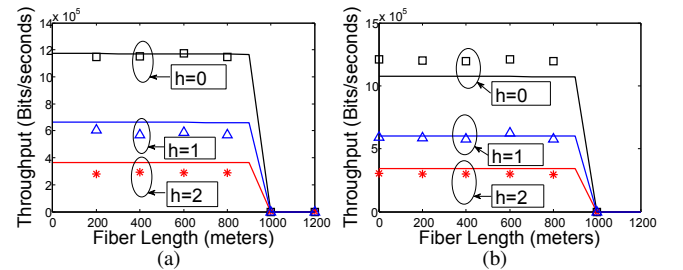


Fig. 9. Individual throughput of contending stations with different fiber length (a) Basic access mechanism, (b) RTS/CTS access mechanism.

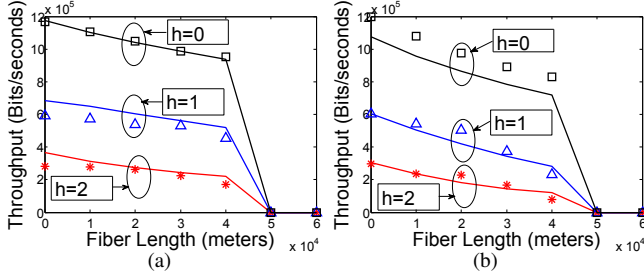


Fig. 10. Individual throughput of contending stations with different fiber length (a) Basic access mechanism, (b) RTS/CTS access mechanism.

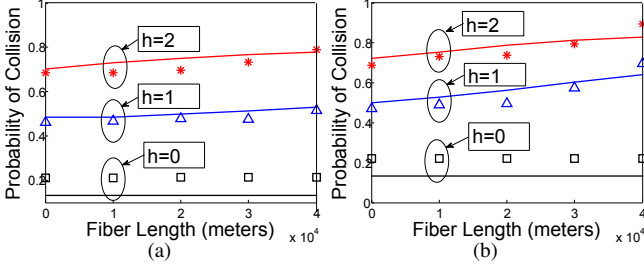


Fig. 11. Probability of collision of contending stations with different fiber length (a) Basic access mechanism, (b) RTS/CTS access mechanism.

C. Effect of Fiber Length

Fig. 9 shows the variation of throughput with different fiber length for both access mechanisms at an offered load of 400 Kbps. It is observed that if the fiber length crosses a maximum limit (for $M = 10 \mu s$, $L < 1000$ meters from equation (24) and (25)), the throughput drops down because of the timeouts. But until that point is reached, the throughput does not change significantly with the fiber length as the propagation delay is insignificant (fiber length < 1000 meters).

To determine the effect of long fiber propagation delays, we change the maximum propagation delay M to $500 \mu s$, shown in Fig. 10. Thus timeouts occur at a fiber length of 50000 meters; however, until then the throughput drops with the fiber length. This is due to the higher contention from the contending stations and higher collision from hidden stations due to increase in vulnerable period because of extra fiber propagation delay. To observe the effect of fiber delay on probability of collision, we vary the fiber length from 0 to 4000 meters and the effect is shown in Fig. 11. It is observed that in the absence of hidden stations, probability of collisions is hardly affected by the fiber delay. However, the situation is different in the presence of hidden stations because of the increase in vulnerable period.

V. CONCLUSION

In this paper, we derive an analytical model to calculate necessary network parameters of a packet for the basic and RTS/CTS access methods in IEEE 802.11 DCF under non-saturation condition in presence of hidden stations for radio-over-fiber LANs. We show the effect of hidden stations and buffer size on different network parameters like throughput,

probability of collision, access delay etc. We also investigate the effect of fiber propagation delay on throughput and probability of collision. The accuracy of our analytical model is also confirmed with extensive simulations.

APPENDIX

A. Calculation of Average Backoff Time

Let us assume that \bar{T}_B^i is the average backoff time at the i -th backoff stage, then

$$\begin{aligned} \bar{T}_B^i &= T \sum_{j=0}^{W_i-1} P\{U_i = j\} j = T \sum_{j=0}^{W_i-1} \frac{j}{W_i} \\ &= \frac{T(W_i - 1)}{2} \end{aligned} \quad (26)$$

where U_i is a random variable with discrete uniform distribution. Now let us assume that the packet is transmitted successfully at the end of the k -th backoff slot. Then the backoff time is given by

$$\bar{T}_B(k) = \sum_{i=1}^k \bar{T}_B^i + (k-1)T_c \quad (27)$$

Let K is the discrete random variable of the number of backoff stages a station has to go through before transmitting a successful packet. Then the probability a packet takes k attempts is $Pr[K = k] = (1-p)p^{k-1}$. Then the average time spent for backoff \bar{T}_B can be given by

$$\begin{aligned} \bar{T}_B &= E\{\bar{T}_B(k)\} = \sum_{k=1}^{\infty} \bar{T}_B(k) P\{K = k\} \\ &= \sum_{k=1}^{\infty} \left[\left(\sum_{i=1}^k \bar{T}_B^i \right) + (k-1)T_c \right] p^{k-1} (1-p) \\ &= \sum_{k=1}^{\infty} \left[\left(\sum_{i=1}^k \frac{T(W_i-1)}{2} \right) + (k-1)T_c \right] p^{k-1} (1-p) \\ &= \sum_{k=1}^{\infty} \left(\sum_{i=1}^k \frac{TW_i}{2} \right) p^{k-1} (1-p) - \frac{T}{2(1-p)} + \frac{p}{1-p} T_c \\ &= \frac{T \left(W_0 \left[\frac{1-p-2^m p^{m+1}}{1-2p} \right] - 1 \right)}{2(1-p)} + \frac{p}{1-p} T_c \end{aligned}$$

REFERENCES

- [1] G. Bianchi, "Performance analysis of the IEEE 802.11 distributed coordination function," *IEEE Journal on Selected Areas in Communications*, vol. 18, pp. 535–547, 2000.
- [2] D. Malone, K. Duffy, and D. Leith, "Modeling the 802.11 distributed coordination function in nonsaturated heterogeneous conditions," *IEEE/ACM Trans. Netw.*, vol. 15, pp. 159–172, February 2007.
- [3] T.-C. Hou, L.-F. Tsao, and H.-C. Liu, "Analyzing the throughput of IEEE 802.11 DCF scheme with hidden nodes," in *Vehicular Technology Conference, 2003. IEEE VTC*, 2003, pp. 2870–2874.
- [4] O. Ekici and A. Yongacoglu, "Modeling hidden terminals in IEEE 802.11 networks," in *PIMRC*, 2008, pp. 1–5.
- [5] M. M. Carvalho and J. J. Garcia-Luna-Aceves, "Delay analysis of IEEE 802.11 in single-hop networks," in *ICNP*, 2003, pp. 146–155.
- [6] P. Chatzimisios, A. C. Boucouvalas, and V. Vitsas, "Packet delay analysis of IEEE 802.11 MAC protocol," *Electronics Letters*, vol. 39, pp. 1358–1359, 2003.
- [7] F.-Y. Hung and I. Marsic, "Access delay analysis of IEEE 802.11 DCF in the presence of hidden stations," in *GLOBECOM*, 2007, pp. 2541–2545.
- [8] K. Duffy and A. J. Ganesh, "Modeling the impact of buffering on 802.11," *IEEE Communications Letters*, vol. 11, pp. 219–221, 2007.
- [9] B. Kalantari-Sabet, M. Mjeku, N. J. Gomes, and J. E. Mitchell, "Performance impairments in single-mode radio-over-fiber systems due to MAC constraints," *J. Lightwave Technol.*, vol. 26, no. 15, pp. 2540–2548, Aug 2008.